Volume 42 | Number 1 | 7 January 2018 | Pages 1–748

NJC

New Journal of Chemistry

A journal for new directions in chemistry

rsc.li/njc

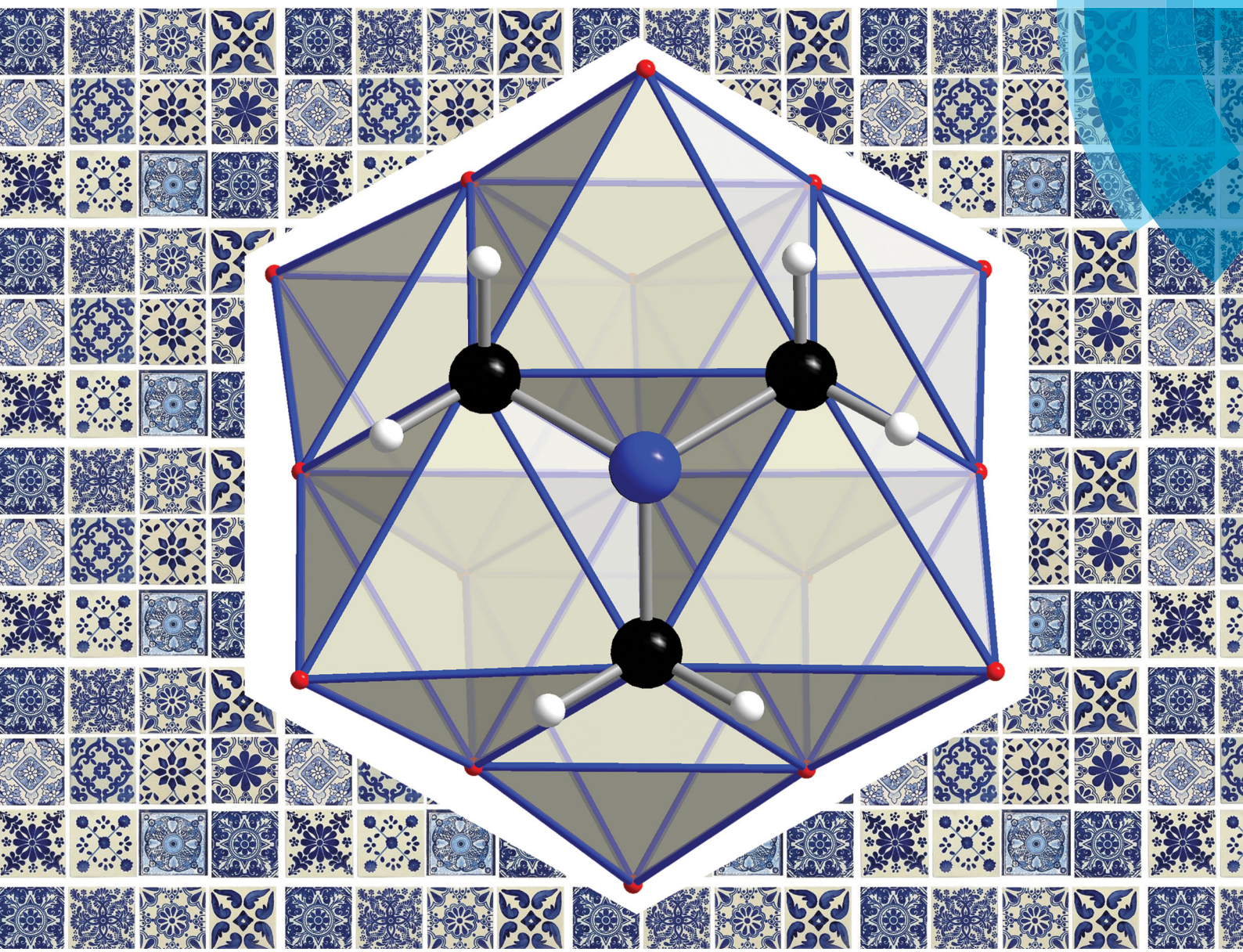

ISSN 1144-0546

ROYAL SOCIETY OF CHEMISTRY

LETTER

H. Karoui and C. Ritchie

Microwave-assisted synthesis of organically functionalized hexa-molybdovanadates

cnrs

NJC

LETTER

View Article Online
View Journal | View Issue

Cite this: *New J. Chem.*, 2018, **42**, 25

Received 1st August 2017,
Accepted 15th November 2017

DOI: 10.1039/c7nj02820b

rsc.li/njc

Microwave-assisted synthesis of organically functionalized hexa-molybdovanadates†

H. Karoui and C. Ritchie *

The microwave-assisted reaction of $(TBA)_4[\beta\text{-}Mo_8O_{24}]$ and $(TBA)_3[H_3V_{10}O_{28}]$ with pentaerythritol or tris(hydroxymethyl)aminomethane yields polyanions with the general formula $(TBA)_2[V_3Mo_3O_{16}(O_3\text{–}R)]$ (R: C_5H_8OH – 1; R: $C_4H_6NH_2$ – 3). Post-synthetic esterification of 1 yields the acylated derivative 2, with all compounds being characterized in the solid and solution state.

Isopolyoxometalates are oligomeric molecular metal oxides with notable structural diversity, while incorporation of heteroatoms into the metal oxide framework in the form of organic,[1] organometallic,[2] main group,[3] transition metal,[4] lanthanoid[5,6] and actinoid[7] components yield heteropolyoxometalates. Consequently, the properties of polyoxometalates (POMs) are equally extensive, resulting in their investigation in research areas encompassing molecular magnetism,[8] catalysis,[9–11] nano-materials,[12,13] energy storage,[14,15] and sensing applications.[16,17]

Modification of POM surfaces by covalently grafting organic ligands has been a long-standing strategy to generate hybrid molecular materials *via* one-pot or post-synthetic methodologies.[18,19] The selection of synthetic approach is driven by the most efficient method to yield analytically pure products due to difficulties associated with the separation of POM mixtures.[20] Post-synthetic modification is therefore most commonly utilized when targeting the introduction of sophisticated organic components that are challenging to cleanly install in one step.[18,19] Despite the impressive range of inorganic–organic hybrids reported to date, the number of polyoxometalate (POM) platforms available for functionalisation is somewhat limited. The most intensively studied alkoxo functionalised POMs include the hexavanadate Lindqvist $[V_6O_{19}\{R\}_2]^{2-}$ and the one and two-sided Anderson-Evans $[M(Mo_6O_{24})\{(OCH_2)_3C\text{–}R\}_1]$, $[M(Mo_6O_{24})\{(OCH_2)_3C\text{–}R\}_2]$ (R = CH_3, NO_2, CH_2OH, NH_2…) species.[21,22] Additionally, the Wells-Dawson phosphovanadotungstates of general formula $[RC(CH_2O)_3V_3P_2W_{15}O_{59}]^{6-}$ (R = CH_3, NO_2, CH_2OH) firstly reported by Hill *et al.* have been utilized as building blocks for structural and compositional diversification.[23] Overall these compounds can generally be prepared in good yield and relatively high purity.

Recently, we reported the initial findings of our investigation targeting the microwave-assisted synthesis of molybdovanadates.[24] As part of that work we discussed the facile preparation of the alkoxo-functionalized molybdovanadate $(TBA)_2[V_3Mo_3O_{16}\{C_5H_9O_3\}]$ from $(TBA)_4[\beta\text{-}Mo_8O_{24}]$, $(TBA)_3[H_3V_{10}O_{28}]$ and tris(hydroxymethyl)-ethane.[24] As a continuation of that study, we established that the methodology could be extended to yield more synthetically useful derivatives.

Herein, we report the microwave-assisted synthesis and characterisation of alcohol, acetyl and amine terminated molybdovanadates of general formula $(TBA)_2[V_3Mo_3O_{16}(O_3\text{–}R)]$; where R = $(C_5H_9O_1)$ **1**, $(C_7H_{11}O_2)$ **2** and (C_4H_8N) **3**. The three compounds are characterised in the solid state by single crystal X-ray diffraction, FT-IR and elemental analysis, meanwhile the solution stability and structural isomer distributions of **1–3** in acetonitrile using ESI-MS, UV-Vis, and NMR spectroscopy are reported.

Compounds **1** and **3** were prepared by reacting $(TBA)_4[\beta\text{-}Mo_8O_{26}]$ and $(TBA)_3[H_3V_{10}O_{28}]$ in acetonitrile with either pentaerythritol (Tris-OH) or tris(hydroxymethyl)aminomethane (Tris-NH_2) respectively, in the stoichiometric ratios found in the products. Microwave irradiation of the reaction mixture for 5 minutes at 110 °C and 4 bar, results in the formation of a dark brown solution that is subsequently purified *via* ether precipitation multiple times to yield crystalline products of **1** and **3** in 56% and 43% yield based on vanadium (see the ESI†). An acylation reaction of compound **1** with acetic anhydride, *N*,*N*-dimethylaminopyridine (DMAP) and triethylamine (TEA) in acetonitrile afforded compound **2** in 11% yield. The compositions of **1–3** were confirmed by ESI-MS (Fig. S11–S13 and Tables S1–S3 in ESI†), with the spectra of each compound containing two distinctive isotopic envelopes that are attributed to the

School of Chemistry, The University of Melbourne, Parkville, Victoria 3010, Australia. E-mail: critchie@unimelb.edu.au

† Electronic supplementary information (ESI) available. CCDC 1553741–1553743. For ESI and crystallographic data in CIF or other electronic format see DOI: 10.1039/c7nj02820b

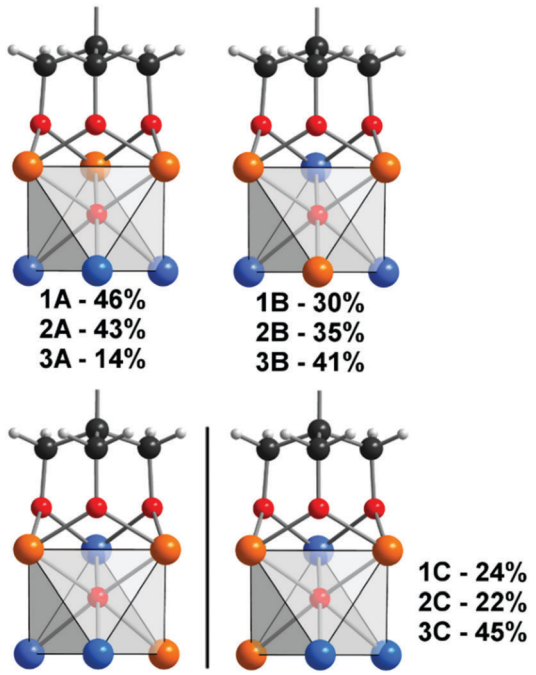

Fig. 1 Simplified mixed polyhedral, ball and stick representation of the structural isomers **A–C** and their distributions for compounds **1–3**. Vanadium, orange spheres; molybdenum, blue spheres; carbon, black spheres; hydrogen, white spheres; oxygen, red spheres.

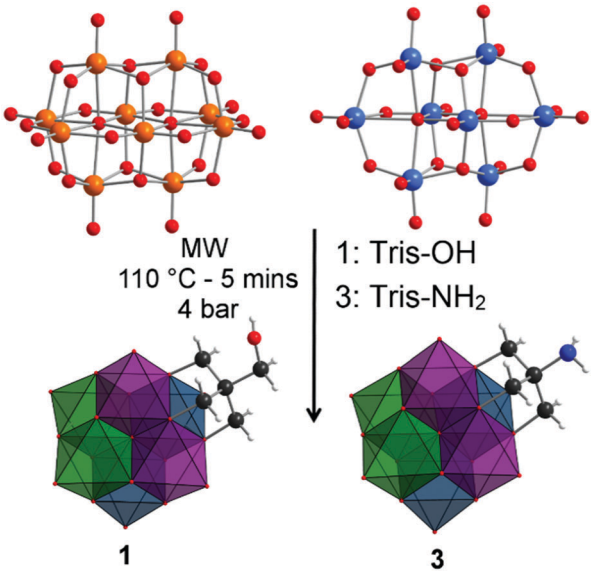

Scheme 1 Synthetic scheme for the preparation of **1** and **3**. Carbon, black spheres; hydrogen, white spheres; nitrogen, blue spheres; molybdenum, light blue spheres; oxygen, red spheres; vanadium, orange spheres. Metal site occupancies: site **A**: V 0.75, Mo 0.25 purple polyhedra; site **B**: V 0.5, Mo 0.5 teal polyhedra; site **C**: V 0.25, Mo 0.75 green polyhedra.

mono- and di-anions of the parent clusters. The mono-anion envelopes for **1–3** are centred at *m*/*z* 1072.52, 1114.64 and 1072.37 respectively.

Crystallographic analysis of **1–3** reveals a mixture of structural isomers as observed for $(TBA)_2[V_3Mo_3O_{16}\{C_5H_9O_3\}]$, with the tripodal ligand being condensed to a vanadium rich triad, ($\{V_3\}$ or $\{V_2Mo_1\}$).[22] This non-random distribution of V and Mo results in the polyanion metal–oxo core having C_{3v} – **1A–3A**, C_s – **1B–3B** or C_1 – **1C–3C** point symmetry (Fig. 1). Despite the inability to distinguish isomers due to the averaging nature of X-ray diffraction, assignment of three distinct crystallographic metal sites with the following occupancies (site **A** – V, 0.75; Mo, 0.25, site **B** – V, 0.5; Mo, 0.5, site **C** – V, 0.25; Mo, 0.75) is possible (Scheme 1). Correspondingly, the metal–oxo bond lengths within the hexametallates can be clearly differentiated for the three crystallographically defined sites **A–C** (Fig. 1, Table 1). As expected the vanadium rich site **A** has the shortest average terminal M–O_t bonds (M–O_t; 1.615 Å), with the corresponding molybdenum rich site **C** having the longest average terminal M–O_t bonds (Mo–O_t; 1.666 Å). The molybdenum rich and ligand free triad ($\{Mo_3\}$ or $\{Mo_2V_1\}$) is somewhat compressed in comparison to the ligand grafted triad. Additional crystallographic details are provided in the ESI† (Table S7).

In addition to the crystallographic comparisons, NMR has proven very informative, with excellent correlation between the experimentally observed and theoretically predicted distribution of structural isomers for $[V_3Mo_3O_{16}(O_3C_5H_9)]^{2-}$, with no structural re-arrangement in MeCN at room temperature. We anticipated that the same distribution and stability would be observed for **1–3**, however, our findings reveal a more complicated situation (Fig. 1). Assignment of the ^{1}H NMR spectrum of freshly prepared samples of **1** and **2** in D_3-acetonitrile revealed the same preferential substitution pattern (**A** > **B** > **C**) as for $[V_3Mo_3O_{16}\{C_5H_9O_3\}]^{2-}$ with slightly higher populations of isomers **B** and **C** (Fig. 1 and Fig. S1, S2, ESI†). Unexpectedly this trend is reversed for the amine terminated polyanion (**3C** > **3B** > **3A**) with the relative populations determined by integration of ^{1}H peak areas (Fig. 1 and Fig. S3, ESI†). The ^{1}H NMR spectra of **1–3** resemble that of the previously reported $[V_3Mo_3O_{16}\{C_5H_9O_3\}]^{2-}$, with deshielded methylene proton resonances between 4.50 and 5.25 ppm being due to their proximity to the electron deficient V^V or Mo^{VI} (Fig. 1 and Tables S4–S6, ESI†). The C_{3v} symmetry of isomers **1A–3A** results in a single resonance for the methylene $-(CH_2)_3$–R protons of the grafted ligand, meanwhile a broad singlet and two sets of broad doublets- are observed for the C_s symmetrical **1B–3B** isomers $-(CH_{A2})(CH_{BC})_2$–R (Fig. S1–S3 and Tables S4–S6, ESI†). The singlet is observed for the two equivalent protons bisected by the mirror plane with the pair of doublets (J = 11.5 Hz) due to coupling between the two diastereotopic geminal protons H_B and H_C (Fig. 2). The meridional arrangement of the V atoms in isomers **1–3C/C′** results in chiral polyanions, where each of the methylene protons are inequivalent. Significant peak overlap complicates the unambiguous assignment of the methylene protons, nonetheless two doublets of doublets with coupling constants of (J = 11.5 Hz and 1.5 Hz) attributed to geminal and 4-bond "W" coupling are clearly identifiable in **2C/C′**. Integration of peak areas associated with the methylene (3.9–4.02 ppm) and methyl (2.83–3.01 ppm) resonances of acetyl functionalised **2** assists with the assignment and relative population of isomers **A–C**.

Cyclic voltammetric analysis of compounds **1–3** in MeCN were conducted to gain some understanding of their

Table 1 Site occupancies and corresponding average bond lengths (Å) of **1–3**. Sites **A–C** are as defined in Scheme 1. O_t – terminal oxo ligand; O_b – μ^2 bridging oxo ligand; O_c – central μ^6 oxo ligand

Compound	Site **A**			Site **B**			Site **C**		
	M–O_t	M–O_b	M–O_c	M–O_t	M–O_b	M–O_c	M–O_t	M–O_b	M–O_c
1	1.615	1.820–2.054	2.231	1.650	1.848–2.012	2.281	1.665	1.921	2.356
2	1.614	1.712–2.087	2.247	1.640	1.812–2.088	2.284	1.664	1.871–1.957	2.299
3	1.615	1.825–2.048	2.228	1.639	1.880–2.090	2.277	1.667	1.921	2.365

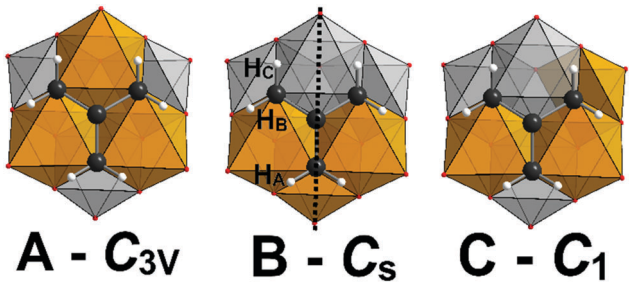

Fig. 2 Mixed polyhedral, ball and stick representation of isomers **A–C** emphasising the methylene proton environments. Vanadium, orange polyhedra; molybdenum, grey polyhedra; carbon, black spheres; hydrogen, white spheres; oxygen, red spheres.

electrochemical properties. All three compounds possess a one-electron quasi-reversible reduction wave (with $E_{1/2}$ = −0.584 V *vs.* Fc/Fc$^+$ for **1**, $E_{1/2}$ = −0.615 V *vs.* Fc/Fc$^+$ for **2** and $E_{1/2}$ = −0.572 V *vs.* Fc/Fc$^+$ for **3**); that we have assigned as reduction of one V^V to V^{VI}, based on previous data reported by Zubieta *et al.* on hexavanadates.[25] Comparison of this redox couple with hexavanadate derivatives indicates a significant electron withdrawing influence of the three electron-deficient Mo^{VI} centres, with the one-electron reduced derivatives of $[V_2{}^{V}V_1{}^{IV}Mo_3O_{16}(OCH_2)_3\text{–}R]^{3-}$ being stabilized with respect to the nitroso derivative of the structurally related hexavanadate $[V_5{}^{V}V_1{}^{IV}O_{13}\{(OCH_2)_3CNO_2\}_2]^{3-}$ in line with the more positive first reduction wave.[25] Furthermore, the insensitivity of the UV-Vis spectra to modifications of the organic ligand is in agreement with this observation, with the lowest lying electronic transition (for **2**, 365 nm, ε = 0.7670 × 10^4 M^{-1} cm^{-1}) being assigned as an LMCT band (Fig. 3).

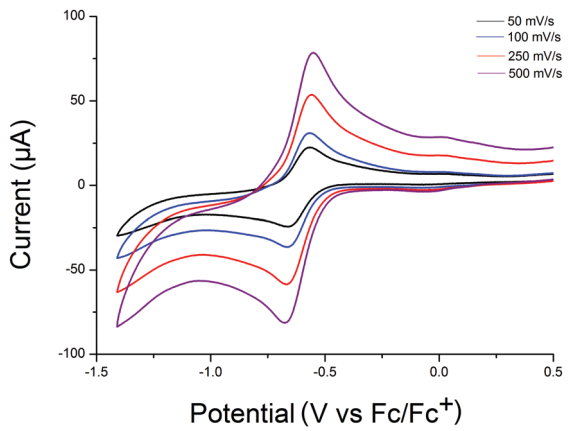

Fig. 3 Cyclic voltammogram of 0.1 mM **2** in a 0.1 M TBA-PF_6 electrolyte solution showing a quasi-reversible one-electron redox process.

In conclusion, we report the extension of our previously established microwave-assisted synthesis of the hexamolybdovanadate $[V_3Mo_3O_{16}\{C_5H_9O_3\}]^{2-}$ to include alcohol **1** and amine **3** terminated derivatives. Post-synthetic derivatization of **1** to yield acetylated **2** verifies that this POM platform holds significant potential as a new building block that can be utilized in a wide range of functional materials. Attempts to separate the isomeric mixtures of these compounds is ongoing.

We thank the Australian Research Council (DE130100615) and the University of Melbourne for financial support.

Conflicts of interest

There are no conflicts to declare.

Notes and references

1 Z. Peng, *Angew. Chem., Int. Ed.*, 2004, **43**, 930–935.
2 B. Artetxe, S. Reinoso, L. San Felices, P. Vitoria, A. Pache, J. Martín-Caballero and J. M. Gutiérrez-Zorrilla, *Inorg. Chem.*, 2015, **54**, 241–252.
3 A. Tézé, M. Michelon and G. Hervé, *Inorg. Chem.*, 1997, **36**, 505–509.
4 H. Lv, J. Song, Y. V. Geletii, J. W. Vickers, J. M. Sumliner, D. G. Musaev, P. Kögerler, P. F. Zhuk, J. Bacsa, G. Zhu and C. L. Hill, *J. Am. Chem. Soc.*, 2014, **136**, 9268–9271.
5 C. Ritchie, V. Baslon, E. G. Moore, C. Reber and C. Boskovic, *Inorg. Chem.*, 2012, **51**, 1142–1151.
6 C. Ritchie, E. G. Moore, M. Speldrich, P. Kögerler and C. Boskovic, *Angew. Chem., Int. Ed.*, 2010, **49**, 7702–7705.
7 S. S. Mal, M. H. Dickman and U. Kortz, *Chem. – A Eur. J.*, 2008, **14**, 9851–9855.
8 S. Cardona-Serra, J. M. Clemente-Juan, E. Coronado, A. Gaita-Ariño, N. Suaud, O. Svoboda, R. Bastardis, N. Guihéry and J. J. Palacios, *Chem. – A Eur. J.*, 2015, **21**, 763–769.
9 S.-S. Wang and G.-Y. Yang, *Chem. Rev.*, 2015, **115**, 4893–4962.
10 H. Lv, Y. V. Geletii, C. Zhao, J. W. Vickers, G. Zhu, Z. Luo, J. Song, T. Lian, D. G. Musaev and C. L. Hill, *Chem. Soc. Rev.*, 2012, **41**, 7572–7589.
11 K. Kastner, A. J. Kibler, E. Karjalainen, J. A. Fernandes, V. Sans and G. N. Newton, *J. Mater. Chem. A*, 2017, **5**, 11577–11581.

12 S. Landsmann, M. Luka and S. Polarz, *Nat. Commun.*, 2012, **3**, 1299.
13 J. Li, X. Li, J. Xu, Y. Wang, L. Wu, Y. Wang, L. Wang, M. Lee and W. Li, *Chem. – A Eur. J.*, 2016, **22**, 15751–15759.
14 S. Herrmann, C. Ritchie and C. Streb, *Dalton Trans.*, 2015, **44**, 7092–7104.
15 S. Herrmann, N. Aydemir, F. Nägele, D. Fantauzzi, T. Jacob, J. Travas-Sejdic and C. Streb, *Adv. Funct. Mater.*, 2017, **27**, 1700881.
16 M. Ortiz, A. M. Debela, M. Svobodova, S. Thorimbert, D. Lesage, R. B. Cole, B. Hasenknopf and C. K. O'Sullivan, *Chem. – Eur. J.*, 2017, **23**, 10597.
17 A. M. Kaczmarek, J. Liu, B. Laforce, L. Vincze, K. Van Hecke and R. Van Deun, *Dalton Trans.*, 2017, **46**, 5781–5785.
18 A. Proust, B. Matt, R. Villanneau, G. Guillemot, P. Gouzerh and G. Izzet, *Chem. Soc. Rev.*, 2012, **41**, 7605–7622.
19 A. Dolbecq, E. Dumas, C. R. Mayer and P. Mialane, *Chem. Rev.*, 2010, **110**, 6009–6048.
20 C. Yvon, A. Macdonell, S. Buchwald, A. J. Surman, N. Follet, J. Alex, D.-L. Long and L. Cronin, *Chem. Sci.*, 2013, **4**, 3810–3817.
21 P. R. Marcoux, B. Hasenknopf, J. Vaissermann and P. Gouzerh, *Eur. J. Inorg. Chem.*, 2003, 2406–2412.
22 D. Hou, G.-S. Kim, K. S. Hagen and C. L. Hill, *Inorg. Chim. Acta*, 1993, **211**, 127–130.
23 Y. Hou and C. L. Hill, *J. Am. Chem. Soc.*, 1993, **115**, 11823–11830.
24 S. Spillane, R. Sharma, A. Zavras, R. Mulder, C. A. Ohlin, L. Goerigk, R. A. J. O'Hair and C. Ritchie, *Angew. Chem., Int. Ed.*, 2017, **56**, 8568–8572.
25 Q. Chen, D. P. Goshorn, C. P. Scholes, X. L. Tan and J. Zubieta, *J. Am. Chem. Soc.*, 1992, **114**, 4667–4681.

